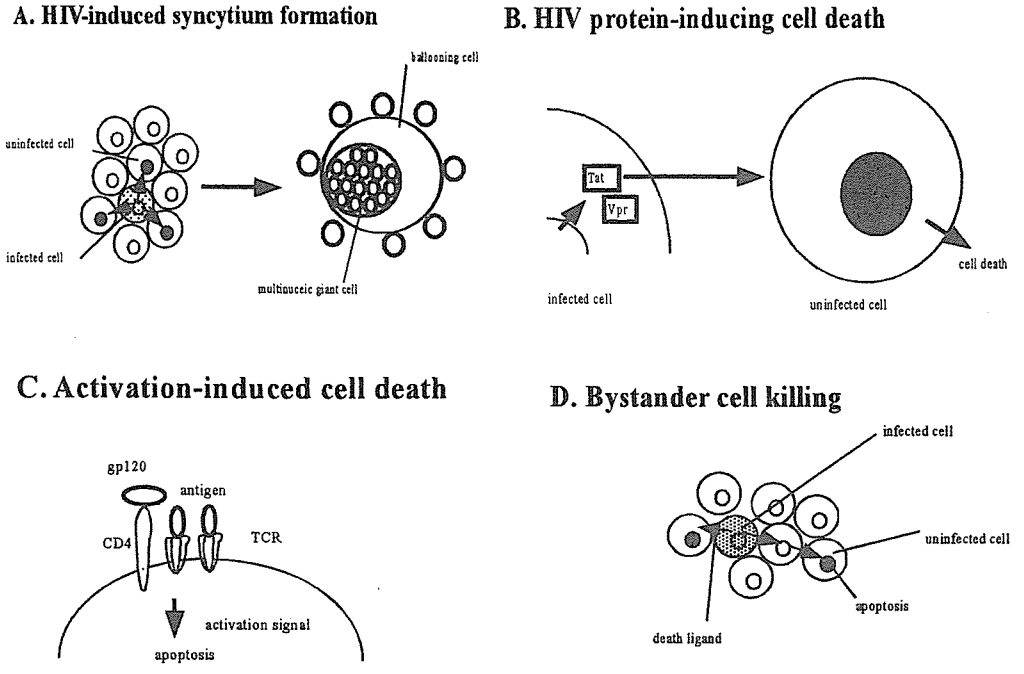

Figure 2. Mechanism of HIV-1-induced cell death. (A) HIV-induced syncytium formation arising from cell to cell fusion. (B) HIV protein-induced cell death. (C) Activation induced cell death through stimulation of TCR or gp120. (D) Bystander cell killing mediated by the death signal

form of caspase 3 efficiently cleaves a variety of cellular constituents, including the DNA repair enzymes, poly-ADP ribose polymerase and DNA-induced protein kinase, cytoskeletal proteins, lamins and actin, and the endonuclease modulator, caspase-activated deoxyribonuclease (CAD) inhibitor (ICAD) [19]. During Fas-mediated apoptosis, the concomitant activation of many other proteins appears to occur. Receptor-interacting protein (RIP), RIP-associated ICH/CED-3-homologous protein with a DD (RAIDD), and procaspase 2 from part of another signaling cascade of the Fas-mediated death pathway were shown to be activated [20]. The activation of the RIP-RAIDD arm of the cell death machinery was demonstrated to serve as a co-stimulator of the FADD-FLICE system [19]. Moreover, upregulation of cytoplasmic DAXX, leading to induction of the stress-activated protein kinase/c-Jun *N*-terminal kinase (SAP/JNK) pathway, represents yet another mechanism by which Fas-mediated apoptosis may occur [21]. The activated form of caspases executes the apoptotic process by cleaving various intracellular substrates leading to genomic DNA fragmentation and resulting in cell membrane blebbing and the exposure of phagocytosis signaling molecules on the cell surface. As mentioned above, FasL-dependent apoptosis plays a critical role in the peripheral elimination of prolongly activated lymphocytes at the end of an immune response [22,23]. Thus, it may be true that FasL has a central role in many of the biological phenomena of activation-induced T-cell apoptosis. In fact, *gld* mice that carry hereditary mutations in the genes encoding FasL are found to suffer from accumulating lymphocytes and a lethal enlargement of lymph nodes. These findings indicate that the main biological role of FasL is to signal the Fas^+ cells to induce instructive apoptosis during the peripheral elimination of lymphocytes. FasL is also expressed in immuno-privileged tissue in which it is difficult to elicit an inflammatory response such as testis and eye [24,25]. FasL may also act as a barrier in the vessel [26]. Significant expression was found on vascular endothelial cells, where it may prevent leukocyte exfiltration into non-inflamed tissues, again by triggering the apoptosis of Fas-expressing leukocytes [27].

TNF, first identified in 1975, is a conventional cytokine and representative of a large superfamily of cytokines that exert physiological roles in cell proliferation, cell death and inflammation as well

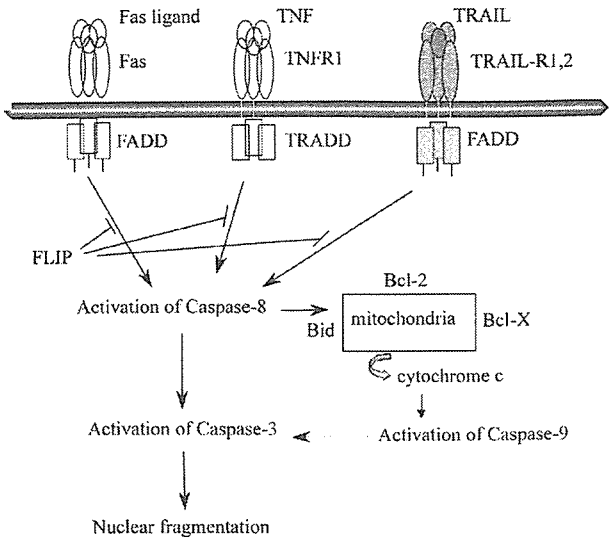

Figure 3. The death ligand-mediated apoptotic pathway. Ligation of the death ligand receptor leads to the formation of DISC comprising the adaptor protein (FADD, TRADD) and procaspase-8 and resulting in the activation of caspase-8. The binding of FLIP to FADD inhibits caspase-8 activation. Caspase-8 can then either directly activate effector caspases (caspase-3) or cleave the proapoptotic Bcl-2 family member Bid. Bid acts with the proapoptotic Bcl-2 family. The involvement of the mitochondria is manifested by the release of cytochrome c into the cytosol where it associates with Apaf-1 and procaspase-9 to form the apoptosome, leading to caspase-9 activation and subsequent caspase-3 activation and nuclear fragmentation

as pathological roles in immunological processes. The best-characterised death receptor is TNFR1. Trimerised TNFR1 can recruit an adaptor molecule, TNFR-associated DD (TRADD), which subsequently recruits FADD and procaspase-8. The intracellular signaling cascade through TNFR1 seems to be more complex than that through Fas. Indeed, in addition to recruiting caspase-activating adaptor molecules, TNFR1 induces the recruitment of many other proteins that engage various signal transduction pathways, some of which either abrogate or potentiate the apoptotic response. For example, TRADD also binds serine-threonine kinase RIP, thereby coupling the stimulation of TNFR1 to the activation of nuclear factor-κB (NF-κB) and offering protection against TNF-induced apoptosis [28]. RIP possesses a functional *N*-terminal kinase domain and can autophosphorylate itself, but this phospharylation does not induce activation of NF-κB. TNF receptor-associated factor 2 (TRAF2) has been likewise implicated in the activation of NF-κB through stimulation of NF-κB-inducing kinase (NIK). However, studies TRAF-2-knockout mice indicated that RIP is most likely responsible for the activation of NF-κB, whereas TRAF2 preferentially activates JNK. TNF knockout mice exhibited increased susceptibility to microbial infection and suppressed inflammatory response when challenged with bacterial endotoxin. These findings together with results obtained *in vitro* suggested that the main biological role of TNF is the induction of inflammatory-response and stress-response genes through the transcription factors AP-1 and NF-κB.

TRAIL was first identified in 1995 based on its sequence homology to other members of the TNF superfamily [29]. TRAIL is also a type 2 transmembrane protein and its highest level of homology is with FasL, exhibiting 28% amino acid identity in the extracellular receptor-binding motif. Two other unique characteristics of TRAIL have been identified. First, TRAIL selectively induces apoptosis both *in vitro* in transformed cells and *in vivo* in tumor cells but not in most normal cells, except thymocytes, neural cells and hepatocytes [30–32]. Second, whereas the expression of other members of the TNF family is tightly regulated and often only transiently induced on activated cells, the transcript of TRAIL was constitutively expressed in some tissues including spleen, lung and prostate [29]. Because the level of TRAIL expression is not consistent with numbers of apoptotic cells, it was assumed that the expression of its cognate receptor would be restricted or alternatively, that apoptosis in only limited cells would be induced under some biological conditions. However, the regulation of TRAIL-induced cell death appears to be more complex than initially thought because five receptors for TRAIL have been identified including two death-inducing receptors (DR4 and DR5), two decoy receptors (DcR1 and DcR2) [33,34], and the secreted TNFR homologue receptor osteoprotegerin [35,36]. The cytoplasmic region of two of these receptors, DR4 and DR5, contains a region with significant homology to the DD of TNFR1 and Fas, and it was confirmed that DR4 and DR5 are able to induce signals for apoptosis [37]. By contrast, DcR2 contains an incomplete DD and so is unable to transduce a death signal [38]. Similarly, DcR1, which unlike the others lacks a cytoplasmic domain and is bound to the cell surface via a glycosyl-phosphatidylinositol (GPI) anchor, does not mediate apoptosis upon ligation [39]. The

activation of caspase has been demonstrated in TRAIL-induced apoptosis *in vitro*. Many of the same caspases involved in Fas and TNF-induced apoptosis were shown to participate in the TRAIL-induced cell death. The activation of death-induced TRAIL-receptors (DR4 and DR5) initiates recruitment of FADD, which in turn directly recruits procaspase-8 to form DISC and results in autoactivation of caspase-8, which then activates downstream effector caspases or the cleaved RIP directly [40]. The NF-κB or JNK signaling pathway was also shown to be activated through DR4 and DR5, respectively, analogous to TNFR1 [41]. It has been suggested that decoy receptors operate to protect normal cells from TRAIL-mediated apoptosis [33,38]. Also, certain intracellular regulatory molecules that control TRAIL-induced apoptosis, such as cFLIP (cellular-FLICE-inhibitory protein), may also operate [42]. Early studies indicated a high level of cFLIP in a TRAIL-resistant melanoma cell line [43]. Furthermore, the level of cFLIP clearly correlated with the sensitivity to TRAIL in some keratinocytes [42]. In addition, it was shown that overexpression of cFLIP frequently causes cells to become resistant to TRAIL because in the presence of cFLIP, procaspase-8 is unable to convert processed caspase-8 generated at the DISC and so remains inactivated [44]. However, inhibition of overall transcription and translation was observed in TRAIL-induced apoptosis without a change in cFLIP levels [45]. These results suggest a significant role for cFLIP in modulating the sensitivity to TRAIL of many cells. It was recently reported that mice deficient in TRAIL exhibit defects of apoptosis in the thymus and develop heightened autoimmune responses, hypersensitivity, to collagen-induced arthritis and streptozotocin-induced diabetes [46]. However, the physiological defect was slighter in the TRAIL-deficient mice than either the FasL- or TNF-deficient mice. Thus, TRAIL seems to have minor physiological roles.

The screening of an EST database revealed another death ligand, called TWEAK [47], whose closest homologue is TNF. Like TNF, TWEAK efficiently promotes apoptosis in certain tumor cell lines and the inhibition of protein synthesis in TWEAK-induced cells further augments apoptosis. TWEAK efficiently activates NF-κB and induces expression of IL-8. Unlike TNF, whose expression is found in activated lymphoid and endothelial cells, the TWEAK transcript was found to be constitutively expressed in many tissues. DR3 was originally identified as a molecule interacting with TNFR1 and reported to be a receptor for TWEAK [48,49]. Similar to TNF-TNFR1 signaling, the activation of DR3 was demonstrated to induce apoptosis as well as the activation of NF-κB and the apoptosis is mediated via interactions with TRADD, FADD and caspase 8, while the activation of NF-κB is induced by a TRADD, TRAF2 and RIP-mediated pathway. However, a high level of TWEAK expression was found in many tissues, whereas DR3 expression was demonstrated to be restricted to peripheral blood lymphocytes (PBLs), thymus, spleen, colon and small intestine [50]. The physiological role of TWEAK remains to be elucidated.

HIV INFECTION AND DEATH LIGANDS

Extensive death ligand-mediated apoptosis is thought to occur in many infectious diseases. Significant augmentation of FasL expression is found in cells expressing hepatitis B and hepatitis C viruses [51,52], although some studies indicated that an increased level of FasL *in vivo* is not associated with HIV disease progression [53,54]. It is remarkable that HIV-1-infected T cells in culture as well as T cells from HIV-infected individuals are highly susceptible to Fas-induced apoptosis [55]. Clinical studies have shown that the expression of Fas as well as the susceptibility to Fas-induced apoptosis increased significantly in cultured $CD4^+$ and $CD8^+$ T cells derived from HIV-1-infected individuals and this high level of Fas expression was positively correlated with disease progression [56]. An increased level of soluble Fas was also found in the plasma of HIV-1-infected individuals and this can be used as a marker for the prognosis of AIDS [57]. FasL was also shown to be upregulated in cultured $CD4^+$ and $CD8^+$ T cells from AIDS patients and, a high level of soluble FasL in serum was found in AIDS patients. Furthermore, FasL expression on macrophages was detected in lymphoid tissue of HIV-1-infected subjects [58]. The observation that retinoic acid inhibits the expression of FasL and the subsequent apoptosis of $CD4^+$ T cells *ex vivo* further supports a causal role for Fas-FasL interactions in the $CD4^+$ T cell death that is induced by HIV infection [59]. Interestingly, the exposure of uninfected monocytes to HIV-1 particles *in vitro* has been

reported to enhance significantly FasL expression, suggesting that HIV-1 can induce Fas-dependent apoptosis through the interaction of monocytes with T cells [60,61]. Furthermore, the crosslinking of the CD4 molecule with HIV-1 gp120 on $CD4^+$ T cells activates the Fas-FasL pathway and Nef-expressing T cells co-express FasL, thereby becoming potential killer cells of uninfected Fas-expressing T cells [62,63]. Similarly, Tat, which is secreted by HIV-infected cells, was shown to upregulate Fas and FasL expression on uninfected cells and enhance their susceptibility to Fas-induced apoptosis [61,64]. Since it is known to be expressed even before integration, Nef may protect infected cells from apoptosis and permit infection in resting cells. Interestingly, significant protection against apoptosis is provided through the downregulation of ASK-1 signaling by Fas-FasL suggesting that Nef acts as an anti-apoptotic protein in the infected cells during its replication [65]. It is also clear that Vpu enhances susceptibility to Fas-induced apoptosis [66]. However, the possible involvement of the Fas/FasL pathway in AICD of $CD4^+$ T cells from HIV-1-infected individuals [67,68] remains controversial. Katsikis *et al.* reported that the AICD cultured $CD4^+$ T cells from HIV-infected patients was Fas-independent [69] and it was shown that neither Fas protein nor biologically active FasL was detectable at significant levels in freshly isolated T cells from HIV-1-infected individuals [54]. In addition, FasL-mediated apoptosis may contribute to the elimination of virus-infected cells by the virus-specific cytotoxic lymphocytes or NK cells [70,71].

Susceptibility to TNF in $CD4^+$ T cells isolated from HIV-infected individuals has also been investigated extensively. Although an early report found that peripheral blood T cells from HIV-positive patients were resistant to apoptosis that was induced by ligation of TNFR [56], a more recent study showed that both $CD4^+$ and $CD8^+$ T cells from HIV-infected individuals were significantly susceptible to TNFR1- and R2-induced apoptosis [72]. The possible contribution of TNFR-mediated apoptosis to $CD8^+$ T cell depletion was implied from the observation that ligation of Env to the CXCR4 coreceptor upregulated the expression of TNFR2 on $CD8^+$ T cells, which became susceptible to death induced by the membrane-bound form of TNF expressed on macrophages [73]. An increased level of TNF was also detected in the serum of symptomatic individuals and clearly high levels of soluble TNFR2 were found to be predictive of HIV disease progression [74].

HIV INFECTION AND TRAIL

Treatment with interferon (IFN) significantly augmented the expression of TRAIL on $CD4^+$ T cells [75], monocytes [76] and dendritic cells (DC) [77]. In addition, infection with measles virus augmented TRAIL expression on DC [78]. Therefore, it is possible that TRAIL is involved in the pathogenesis of HIV. In fact, TRAIL, but not FasL-dependent AICD, was detected in $CD4^+$ T cells isolated from HIV-1-infected individuals *in vitro* [79,80]. TRAIL might contribute to a constructive apoptosis of virus-infected cells because T cells from HIV-1-infected patients were more susceptible to the induction of apoptosis by this ligand than uninfected cells, suggesting that TRAIL is involved in HIV-associated T-cell apoptosis [79]. In fact, AICD in $CD4^+$ T cells isolated from HIV-1-infected individuals was inhibited by antagonistic TRAIL-specific antibodies [80]. Furthermore, using an HIV-1-infected mouse model, a significant level of TRAIL-dependent apoptosis in uninfected $CD4^+$ T cells was found. The spleen tissue of hu-PBL-NOD-SCID mice was investigated following infection with HIV-1 and large numbers of $TUNEL^+$ $CD4^+$ cells were found mainly in uninfected cells. The number of $TUNEL^+$ cells was clearly inhibited after administration of anti-TRAIL but not anti-FasL antibody, suggesting that TRAIL is a major death ligand in HIV-1-infected tissues [81,82]. Following infection with HIV-1, Tat protein is released by macrophages or monocytes and seems to upregulate the expression of TRAIL on macrophages as shown by Zhang, indicating that TRAIL-dependent cell death occurs in bystander $CD4^+$ T cells, perhaps triggered by Tat produced from HIV-1-infected cells [83,84].

It is likely that TRAIL is primarily responsible for the apoptosis of bystander $CD4^+$ T cells in HIV-infected lymphoid organs. However, several issues remain to be resolved. First, the mechanism by which HIV-1 infection induces the expression of TRAIL in $CD4^+$ T cells remains to be determined. It was found that the number of $TRAIL^+$ cells was consistently higher in HIV-1-infected mice than uninfected mice. A similar upregulation of TRAIL expression with HIV-1 infection was observed especially on HIV-1-infected

macrophages [85]. The expression of TRAIL on T cells is induced by a variety of stimuli, including type I IFNs and TCR-mediated signals [75,86,87]. Thus it can be postulated that TRAIL was induced to express on HIV-1-uninfected $CD4^+$ T cells by viral or cellular factors from either HIV-1-infected or bystander cells in HIV-1-infected lymphoid organs. Second, it is necessary to determine the receptor molecule involved in TRAIL-mediated apoptosis. It is not yet clear which receptor contributes to this phenomenon. In other viral infections, viral proteins regulate the expression of these receptors. In adenovirus, E3 downregulates its receptor DR4 and DR5 [88]. In respiratory syncytial virus, infection strongly upregulated DR4 and DR5 expression [89]. In HIV infection, Tat and gp120 seem to upregulate DR4 and DR5 expression.

TRAIL seems to be one of the most significant molecules in HIV infection [81,85,90]. This ligand was predominantly expressed on macrophages and monocytes after HIV-1 infection, and was able to induce apoptosis in neurons *in vitro* and *in vivo*, which might explain the neuronal death in HIV-encephalopathy. Recently, a murine model of HIV-encephalopathy was developed and it was found that neuronal apoptosis was significantly induced by TRAIL expressed on HIV-infected macrophages [85]. Furthermore, neuronal apoptosis was confirmed in the brain tissue of HIV-1-encephalopathy patients and cells cultured *in vitro* [90,91]. It is possible that TRAIL has a central role in disease progression in some virus-induced diseases.

CONCLUSION

Although the mechanism of the apoptosis in HIV-infected individuals is likely to be multifactorial, its induction is a critical event *in vivo*. The death ligands in HIV infection are important for this apoptosis in addition to mitochondria-mediated apoptosis. A novel immune-based therapy for modulating the apoptosis in HIV infection is awaited.

ACKNOWLEDGEMENTS

The authors thanks the many scientists who have helped with their work over the years, especially N. Yamamoto and H. Mizusawa for discussions. Research in the authors' laboratory is supported by grants from the Ministry of Health, Labor, and Welfare and the Ministry of Education, Culture, Sports, Science, and Technology of Japan.

REFERENCES

1. Badley AD, Roumier T, Lum JJ, *et al.* Mitochondrion-mediated apoptosis in HIV-1 infection. *Trends Pharmacol Sci* 2003; **24**: 298–305.
2. Arnoult D, Petit F, Lelievre JD, *et al.* Mitochondria in HIV-1-induced apoptosis. *Biochem Biophys Res Commun* 2003; **304**: 561–574.
3. Lifson JD, Reyes GR, McGrath MS, *et al.* AIDS retrovirus induced cytopathology: giant cell formation and involvement of CD4 antigen. *Science* 1986; **232**: 1123–1127.
4. Terai C, Kornbluth RS, Pauza CD, *et al.* Apoptosis as a mechanism of cell death in cultured T lymphoblasts acutely infected with HIV-1. *J Clin Invest* 1991; **87**: 1710–1715.
5. Rinfret A, Latendresse H, Lefebvre R, *et al.* Human immunodeficiency virus-infected multinucleated histiocytes in oropharyngeal lymphoid tissues from two asymptomatic patients. *Am J Pathol* 1991; **138**: 421–426.
6. Frankel SS, Wenig BM, Burke AP, *et al.* Replication of HIV-1 in dendritic cell-derived syncytia at the mucosal surface of the adenoid. *Science* 1996; **272**: 115–117.
7. Sodroski J, Goh WC, Rosen C, *et al.* Role of the HTLV-III/LAV envelope in syncytium formation and cytopathicity. *Nature* 1986; **322**: 470–474.
8. Ferri KF, Jacotot E, Blanco J, *et al.* Apoptosis control in syncytia induced by the HIV type 1-envelope glycoprotein complex: role of mitochondria and caspases. *J Exp Med* 2000; **192**: 1081–1092.
9. Castedo M, Roumier T, Blanco J, *et al.* Sequential involvement of Cdk1, mTOR and p53 in apoptosis induced by the HIV-1 envelope. *EMBO J* 2002; **21**: 4070–4080.
10. Sastry KJ, Marin MC, Nehete PN, *et al.* Expression of human immunodeficiency virus type I tat results in down-regulation of bcl-2 and induction of apoptosis in hematopoietic cells. *Oncogene* 1996; **13**: 487–493.
11. Bartz SR, Emerman M. Human immunodeficiency virus type 1 Tat induces apoptosis and increases sensitivity to apoptotic signals by up-regulating FLICE/caspase-8. *J Virol* 1999; **73**: 1956–1963.
12. Jacotot E, Ravagnan L, Loeffler M, *et al.* The HIV-1 viral protein R induces apoptosis via a direct effect on the mitochondrial permeability transition pore. *J Exp Med* 2000; **191**: 33–46.
13. Green DR, Droin N, Pinkoski M. Activation-induced cell death in T cells. *Immunol Rev* 2003; **193**: 70–81.
14. Muro-Cacho CA, Pantaleo G, Fauci AS. Analysis of apoptosis in lymph nodes of HIV-infected persons. Intensity of apoptosis correlates with the general state of activation of the lymphoid tissue and not

with stage of disease or viral burden. *J Immunol* 1995; **154**: 5555–5566.
15. Finkel TH, Tudor-Williams G, Banda NK, *et al.* Apoptosis occurs predominantly in bystander cells and not in productively infected cells of HIV- and SIV-infected lymph nodes. *Nat Med* 1995; **1**: 129–134.
16. Suda T, Takahashi T, Golstein P, *et al.* Molecular cloning and expression of the Fas ligand, a novel member of the tumor necrosis factor family. *Cell* 1993; **75**: 1169–1178.
17. Medema JP, Scaffidi C, Kischkel FC, *et al.* FLICE is activated by association with the CD95 death-inducing signaling complex (DISC). *EMBO J* 1997; **16**: 2794–2804.
18. Medema JP, Toes RE, Scaffidi C, *et al.* Cleavage of FLICE (caspase-8) by granzyme B during cytotoxic T lymphocyte-induced apoptosis. *Eur J Immunol* 1997; **27**: 3492–3498.
19. Cohen GM. Caspases: the executioners of apoptosis. *Biochem J* 1997; **326**: 1–16.
20. Duan H, Dixit VM. RAIDD is a new 'death' adaptor molecule. *Nature* 1997; **385**: 86–89.
21. Yang X, Khosravi-Far R, Chang HY, *et al.* Daxx, a novel Fas-binding protein that activates JNK and apoptosis. *Cell* 1997; **89**: 1067–1076.
22. Sharma K, Wang RX, Zhang LY, *et al.* Death the Fas way: regulation and pathophysiology of CD95 and its ligand. *Pharmacol Ther* 2000; **88**: 333–347.
23. Newell MK, Desbarats J. Fas ligand: receptor or ligand? *Apoptosis* 1999; **4**: 311–315.
24. Bellgrau D, Gold D, Selawry H, *et al.* A role for CD95 ligand in preventing graft rejection. *Nature* 1995; **377**: 630–632.
25. Griffith TS, Brunner T, Fletcher SM, *et al.* Fas ligand-induced apoptosis as a mechanism of immune privilege. *Science* 1995; **270**: 1189–1192.
26. Walsh K, Sata M. Negative regulation of inflammation by Fas ligand expression on the vascular endothelium. *Trends Cardiovasc Med* 1999; **9**: 34–41.
27. Liles WC, Kiener PA, Ledbetter JA, *et al.* Differential expression of Fas (CD95) and Fas ligand on normal human phagocytes: implications for the regulation of apoptosis in neutrophils. *J Exp Med* 1996; **184**: 429–440.
28. Hsu H, Xiong J, Goeddel DV. The TNF receptor 1-associated protein TRADD signals cell death and NF-kappa B activation. *Cell* 1995; **81**: 495–504.
29. Wiley SR, Schooley K, Smolak PJ, *et al.* Identification and characterization of a new member of the TNF family that induces apoptosis. *Immunity* 1995; **3**: 673–682.
30. Cretney E, Uldrich AP, Berzins SP, *et al.* Normal thymocyte negative selection in TRAIL-deficient mice. *J Exp Med* 2003; **198**: 491–496.
31. Nitsch R, Bechmann I, Deisz RA, *et al.* Human brain-cell death induced by tumour-necrosis-factor-related apoptosis-inducing ligand (TRAIL). *Lancet* 2000; **356**: 827–828.
32. Mori E, Thomas M, Motoki K, *et al.* Human normal hepatocytes are susceptible to apoptosis signal mediated by both TRAIL-R1 and TRAIL-R2. *Cell Death Differ* 2004; **11**: 203–207.
33. Pan G, Ni J, Wei YF, *et al.* An antagonist decoy receptor and a death domain-containing receptor for TRAIL. *Science* 1997; **277**: 815–818.
34. Walczak H, Degli-Esposti MA, Johnson RS, *et al.* TRAIL-R2: a novel apoptosis-mediating receptor for TRAIL. *EMBO J* 1997; **16**: 5386–5397.
35. Almasan A, Ashkenazi A. Apo2L/TRAIL: apoptosis signaling, biology, and potential for cancer therapy. *Cytokine Growth Factor Rev* 2003; **14**: 337–348.
36. MacFarlane M. TRAIL-induced signalling and apoptosis. *Toxicol Lett* 2003; **139**: 89–97.
37. Pan G, O'Rourke K, Chinnaiyan AM, *et al.* The receptor for the cytotoxic ligand TRAIL. *Science* 1997; **276**: 111–113.
38. Sheridan JP, Marsters SA, Pitti RM, *et al.* Control of TRAIL-induced apoptosis by a family of signaling and decoy receptors. *Science* 1997; **277**: 818–821.
39. Legembre P, Moreau P, Daburon S, *et al.* Potentiation of Fas-mediated apoptosis by an engineered glycosylphosphatidylinositol-linked Fas. *Cell Death Differ* 2002; **9**: 329–339.
40. Kischkel FC, Lawrence DA, Chuntharapai A, *et al.* Apo2L/TRAIL-dependent recruitment of endogenous FADD and caspase-8 to death receptors 4 and 5. *Immunity* 2000; **12**: 611–620.
41. Lin Y, Devin A, Cook A, *et al.* The death domain kinase RIP is essential for TRAIL (Apo2L)-induced activation of IkappaB kinase and c-Jun *N*-terminal kinase. *Mol Cell Biol* 2000; **20**: 6638–6645.
42. Leverkus M, Neumann M, Mengling T, *et al.* Regulation of tumor necrosis factor-related apoptosis-inducing ligand sensitivity in primary and transformed human keratinocytes. *Cancer Res* 2000; **60**: 553–559.
43. Griffith TS, Chin WA, Jackson GC, *et al.* Intracellular regulation of TRAIL-induced apoptosis in human melanoma cells. *J Immunol* 1998; **161**: 2833–2840.
44. MacFarlane M, Harper N, Snowden RT, *et al.* Mechanisms of resistance to TRAIL-induced apoptosis in primary B cell chronic lymphocytic leukaemia. *Oncogene* 2002; **21**: 6809–6818.
45. Ahmad M, Shi Y. TRAIL-induced apoptosis of thyroid cancer cells: potential for therapeutic intervention. *Oncogene* 2000; **19**: 3363–3371.
46. Lamhamedi-Cherradi SE, Zheng SJ, Maguschak KA, *et al.* Defective thymocyte apoptosis and accelerated autoimmune diseases in TRAIL-/- mice. *Nat Immunol* 2003; **4**: 255–260.

47. Chicheportiche Y, Bourdon PR, Xu H, *et al.* TWEAK, a new secreted ligand in the tumor necrosis factor family that weakly induces apoptosis. *J Biol Chem* 1997; **272**: 32401–32410.
48. Kitson J, Raven T, Jiang YP, *et al.* A death-domain-containing receptor that mediates apoptosis. *Nature* 1996; **384**: 372–375.
49. Marsters SA, Sheridan JP, Pitti RM, *et al.* Identification of a ligand for the death-domain-containing receptor Apo3. *Curr Biol* 1998; **8**: 525–528.
50. Chinnaiyan AM, O'Rourke K, Yu GL, *et al.* Signal transduction by DR3, a death domain-containing receptor related to TNFR-1 and CD95. *Science* 1996; **274**: 990–992.
51. Yoo YG, Lee MO. Hepatitis B virus X protein induces expression of Fas ligand gene through enhancing transcriptional activity of early growth response factor. *J Biol Chem* 2004; **279**: 36242–36249.
52. Ruggieri A, Murdolo M, Rapicetta M. Induction of FAS ligand expression in a human hepatoblastoma cell line by HCV core protein. *Virus Res* 2003; **97**: 103–110.
53. Vasilescu A, Heath SC, Diop G, *et al.* Genomic analysis of Fas and FasL genes and absence of correlation with disease progression in AIDS. *Immunogenetics* 2004; **56**: 56–60.
54. Sieg S, Smith D, Yildirim Z, *et al.* Fas ligand deficiency in HIV disease. *Proc Natl Acad Sci USA* 1997; **94**: 5860–5865.
55. Ohnimus H, Heinkelein M, Jassoy C. Apoptotic cell death upon contact of CD4+ T lymphocytes with HIV glycoprotein-expressing cells is mediated by caspases but bypasses CD95 (Fas/Apo-1) and TNF receptor 1. *J Immunol* 1997; **159**: 5246–5252.
56. Katsikis PD, Wunderlich ES, Smith CA, *et al.* Fas antigen stimulation induces marked apoptosis of T lymphocytes in human immunodeficiency virus-infected individuals. *J Exp Med* 1995; **181**: 2029–2036.
57. Medrano FJ, Leal M, Arienti D, *et al.* Tumor necrosis factor beta and soluble APO-1/Fas independently predict progression to AIDS in HIV-seropositive patients. *AIDS Res Hum Retroviruses* 1998; **14**: 835–843.
58. Dockrell DH, Badley AD, Villacian JS, *et al.* The expression of Fas Ligand by macrophages and its upregulation by human immunodeficiency virus infection. *J Clin Invest* 1998; **101**: 2394–2405.
59. Yang Y, Bailey J, Vacchio MS, *et al.* Retinoic acid inhibition of *ex vivo* human immunodeficiency virus-associated apoptosis of peripheral blood cells. *Proc Natl Acad Sci USA* 1995; **92**: 3051–3055.
60. Badley AD, McElhinny JA, Leibson PJ, *et al.* Upregulation of Fas ligand expression by human immunodeficiency virus in human macrophages mediates apoptosis of uninfected T lymphocytes. *J Virol* 1996; **70**: 199–206.
61. Westendorp MO, Frank R, Ochsenbauer C, *et al.* Sensitization of T cells to CD95-mediated apoptosis by HIV-1 Tat and gp120. *Nature* 1995; **375**: 497–500.
62. Banda NK, Bernier J, Kurahara DK, *et al.* Crosslinking CD4 by human immunodeficiency virus gp120 primes T cells for activation-induced apoptosis. *J Exp Med* 1992; **176**: 1099–1106.
63. Zauli G, Gibellini D, Secchiero P, *et al.* Human immunodeficiency virus type 1 Nef protein sensitizes CD4(+) T lymphoid cells to apoptosis via functional upregulation of the CD95/CD95 ligand pathway. *Blood* 1999; **93**: 1000–1010.
64. Li CJ, Friedman DJ, Wang C, *et al.* Induction of apoptosis in uninfected lymphocytes by HIV-1 Tat protein. *Science* 1995; **268**: 429–431.
65. Geleziunas R, Xu W, Takeda K, *et al.* HIV-1 Nef inhibits ASK1-dependent death signalling providing a potential mechanism for protecting the infected host cell. *Nature* 2001; **410**: 834–838.
66. Casella CR, Rapaport EL, Finkel TH. Vpu increases susceptibility of human immunodeficiency virus type 1-infected cells to fas killing. *J Virol* 1999; **73**: 92–100.
67. Baumler CB, Bohler T, Herr I, *et al.* Activation of the CD95 (APO-1/Fas) system in T cells from human immunodeficiency virus type-1-infected children. *Blood* 1996; **88**: 1741–1746.
68. Estaquier J, Tanaka M, Suda T, *et al.* Fas-mediated apoptosis of CD4+ and CD8+ T cells from human immunodeficiency virus-infected persons: differential *in vitro* preventive effect of cytokines and protease antagonists. *Blood* 1996; **87**: 4959–4966.
69. Katsikis PD, Garcia-Ojeda ME, Wunderlich ES, *et al.* Activation-induced peripheral blood T cell apoptosis is Fas independent in HIV-infected individuals. *Int Immunol* 1996; **8**: 1311–1317.
70. Petrovas C, Mueller YM, Katsikis PD. HIV-specific CD8+ T cells: serial killers condemned to die? *Curr HIV Res* 2004; **2**: 153–162.
71. Lum JJ, Schnepple DJ, Nie Z, *et al.* Differential effects of interleukin-7 and interleukin-15 on NK cell anti-human immunodeficiency virus activity. *J Virol* 2004; **78**: 6033–6042.
72. de Oliveira Pinto LM, Garcia S, Lecoeur H, *et al.* Increased sensitivity of T lymphocytes to tumor necrosis factor receptor 1 (TNFR1)- and TNFR2-mediated apoptosis in HIV infection: relation to expression of Bcl-2 and active caspase-8 and caspase-3. *Blood* 2002; **99**: 1666–1675.
73. Herbein G, Mahlknecht U, Batliwalla F, *et al.* Apoptosis of CD8+ T cells is mediated by macrophages through interaction of HIV gp120 with chemokine receptor CXCR4. *Nature* 1998; **395**: 189–194.

74. Zangerle R, Gallati H, Sarcletti M, *et al.* Tumor necrosis factor alpha and soluble tumor necrosis factor receptors in individuals with human immunodeficiency virus infection. *Immunol Lett* 1994; **41**: 229–234.
75. Kayagaki N, Yamaguchi N, Nakayama M, *et al.* Type I interferons (IFNs) regulate tumor necrosis factor-related apoptosis-inducing ligand (TRAIL) expression on human T cells: a novel mechanism for the antitumor effects of type I IFNs. *J Exp Med* 1999; **189**: 1451–1460.
76. Griffith TS, Wiley SR, Kubin MZ, *et al.* Monocyte-mediated tumoricidal activity via the tumor necrosis factor-related cytokine, TRAIL. *J Exp Med* 1999; **189**: 1343–1354.
77. Sedger LM, Shows DM, Blanton RA, *et al.* IFN-gamma mediates a novel antiviral activity through dynamic modulation of TRAIL and TRAIL receptor expression. *J Immunol* 1999; **163**: 920–926.
78. Vidalain PO, Azocar O, Lamouille B, *et al.* Measles virus induces functional TRAIL production by human dendritic cells. *J Virol* 2000; **74**: 556–559.
79. Jeremias I, Herr I, Boehler T, *et al.* TRAIL/Apo-2-ligand-induced apoptosis in human T cells. *Eur J Immunol* 1998; **28**: 143–152.
80. Katsikis PD, Garcia-Ojeda ME, Torres-Roca JF, *et al.* Interleukin-1 beta converting enzyme-like protease involvement in Fas-induced and activation-induced peripheral blood T cell apoptosis in HIV infection. TNF-related apoptosis-inducing ligand can mediate activation-induced T cell death in HIV infection. *J Exp Med* 1997; **186**: 1365–1372.
81. Miura Y, Misawa N, Maeda N, *et al.* Critical contribution of tumor necrosis factor-related apoptosis-inducing ligand (TRAIL) to apoptosis of human CD4+ T cells in HIV-1-infected hu-PBL-NOD-SCID mice. *J Exp Med* 2001; **193**: 651–660.
82. Lum JJ, Pilon AA, Sanchez-Dardon J, *et al.* Induction of cell death in human immunodeficiency virus-infected macrophages and resting memory CD4 T cells by TRAIL/Apo2l. *J Virol* 2001; **75**: 11128–11136.
83. Zhang M, Li X, Pang X, *et al.* Identification of a potential HIV-induced source of bystander-mediated apoptosis in T cells: upregulation of trail in primary human macrophages by HIV-1 tat. *J Biomed Sci* 2001; **8**: 290–296.
84. Yang Y, Tikhonov I, Ruckwardt TJ, *et al.* Monocytes treated with human immunodeficiency virus Tat kill uninfected CD4(+) cells by a tumor necrosis factor-related apoptosis-induced ligand-mediated mechanism. *J Virol* 2003; **77**: 6700–6708.
85. Miura Y, Koyanagi Y, Mizusawa H. TNF-related apoptosis-inducing ligand (TRAIL) induces neuronal apoptosis in HIV-encephalopathy. *J Med Dent Sci* 2003; **50**: 17–25.
86. Martinez-Lorenzo MJ, Anel A, Gamen S, *et al.* Activated human T cells release bioactive Fas ligand and APO2 ligand in microvesicles. *J Immunol* 1999; **163**: 1274–1281.
87. Musgrave BL, Phu T, Butler JJ, *et al.* Murine TRAIL (TNF-related apoptosis inducing ligand) expression induced by T cell activation is blocked by rapamycin, cyclosporin A, and inhibitors of phosphatidylinositol 3-kinase, protein kinase C, and protein tyrosine kinases: evidence for TRAIL induction via the T cell receptor signaling pathway. *Exp Cell Res* 1999; **252**: 96–103.
88. Tollefson AE, Toth K, Doronin K, *et al.* Inhibition of TRAIL-induced apoptosis and forced internalization of TRAIL receptor 1 by adenovirus proteins. *J Virol* 2001; **75**: 8875–8887.
89. Kotelkin A, Prikhod'ko EA, Cohen JI, *et al.* Respiratory syncytial virus infection sensitizes cells to apoptosis mediated by tumor necrosis factor-related apoptosis-inducing ligand. *J Virol* 2003; **77**: 9156–9172.
90. Miura Y, Misawa N, Kawano Y, *et al.* Tumor necrosis factor-related apoptosis-inducing ligand induces neuronal death in a murine model of HIV central nervous system infection. *Proc Natl Acad Sci USA* 2003; **100**: 2777–2782.
91. Ryan LA, Peng H, Erichsen DA, *et al.* TNF-related apoptosis-inducing ligand mediates human neuronal apoptosis: links to HIV-1-associated dementia. *J Neuroimmunol* 2004; **148**: 127–139.

Human Reproduction Vol.20, No.6 pp. 1477–1484, 2005
Advance Access publication February 25, 2005
doi:10.1093/humrep/deh783

Reproduction of menstrual changes in transplanted human endometrial tissue in immunodeficient mice

Rui Matsuura-Sawada[1,4], Takashi Murakami[1], Yuka Ozawa[1], Hiroshi Nabeshima[1], Jun-ichi Akahira[1], Yumi Sato[1], Yoshio Koyanagi[2], Mamoru Ito[3], Yukihiro Terada[1] and Kunihiro Okamura[1]

[1]Tohoku University Graduate School of Medicine – Obstetrics and Gynecology, Seiryo-machi1-1, Aoba-ku, Sendai Japan, [2]Virus Research, Kyoto University – Laboratory of Viral Pathogenesis, Kyoto and [3]Central Institute for Experimental Animals, Kawasaki, Japan

[4]To whom correspondence should be addressed. E-mail: sawada@ob-gy.med.tohoku.ac.jp

BACKGROUND: Cultures of human endometrial tissue are useful for analysing the mechanisms underlying the menstrual cycle. However, long-term culture of endometrial tissue is difficult *in vitro*. Xenotransplantation of normal human endometrial tissue into immunodeficient mice could allow prolonged survival of the transplanted tissues. METHODS: Proliferative-phase endometrial tissue samples from three women were transplanted into the subcutaneous space of ovariectomized, immunodeficient, non-obese diabetic (NOD)/severe combined immunodeficiency (SCID)/γC^{null} (NOG) mice. The mice were treated with 17β-estradiol (E_2) for the first 14 days after transplantation, followed by E_2 plus progesterone for the next 14 days. The transplants were investigated morphologically and immunohistochemically at various times after implantation. RESULTS: The transplanted tissues contained large numbers of small glands, pseudostratification of the nuclei and dense stroma after treatment with E_2 alone. After treatment with E_2 plus progesterone, subnuclear vacuolation, luminal secretion and decidualization of the stroma were observed. When the hormone treatment ceased, tissue destruction occurred and the transplants returned to the proliferative phase. Lymphocytes were identified immunohistochemically: the numbers of CD56-positive and CD16-negative cells increased significantly in the stroma during the late secretory phase (day 28). CONCLUSIONS: Human endometrial tissue transplanted into NOG mice showed similar histological changes to eutopic endometrial tissue during treatment with sex steroid hormones for 1 month. Moreover, lymphocytes were produced in the transplanted human endometrial tissue. This system represents a new experimental model of the human endometrium *in vivo*.

Key words: endometrial transplants/human endometrium/immunodeficient mouse model/menstrual cycle

Introduction

Endometrial tissue undergoes periodic cycles of proliferation, differentiation and degeneration that are precisely controlled by sex steroid hormones produced in the ovaries. If fertilization does not occur during a cycle, the cells of the endometrium degenerate and slough off, and the organ prepares itself for nidation in the next cycle. These tissue dynamics have, so far, been difficult to reproduce in experimental models. Therefore, the exact mechanisms that are responsible for these processes are poorly understood.

In 1908, the earliest comprehensive description of the cyclical histological changes that occur in the human endometrium was published (Hitschmann and Adler, 1908). Subsequently, Noyes and colleagues described several histological features that are still used today as criteria for endometrial dating: gland mitoses, pseudostratification of the nuclei, subnuclear vacuolation, gland secretion, stromal oedema, stromal mitoses, pseudodecidual reactions and leukocytic infiltration (Noyes *et al.*, 1950). Although these histological changes have been used widely in clinical diagnosis, their implications are not yet fully understood.

To understand the mechanisms of reproduction, it is essential to establish experimental models of the endometrium throughout the menstrual cycle. Many experiments have examined the mechanism of action of steroid hormones on the endometrium in laboratory animals (Jensen and Jacobson, 1962; O'Mally *et al.*, 1970; Flickinger *et al.*, 1977). However, in mature mice and rats, the reproductive cycle is only 4 or 5 days long and decidualization does not occur unless it is triggered by implantation or stimulated by pregnancy (Finn *et al.*, 1992). Similarly, natural ovulation does not occur in mature rabbits unless mating has occurred. Menstruation occurs only in a very limited number of species: humans, a few Old World primates and a few bats. However, there are significant differences between, for example, rhesus monkeys and humans, in terms of the changes that occur in the endometrium at

implantation (Heuser *et al.*, 1945) and the distribution of the aortic branches supplying the uterus (Nelson, 1964). The reproductive cycle, biochemical responses and mechanisms of menstruation clearly differ between species. Therefore, the results of studies in laboratory animals have been difficult to apply directly to humans.

There have been several studies of the human endometrium using *in vitro* endometrial stroma and/or glandular cell cultures over the past two decades (Centola *et al.*, 1984; Irwin *et al.*, 1989; Sugawara *et al.*, 1997). Although these studies have produced many interesting findings, they may not accurately reflect the events that occur *in vivo*. Tissue culture is a useful method for biochemical and histological analyses. However, it is difficult to culture human endometrial tissue over long periods of time—bearing in mind the 1-month duration of each menstrual cycle—in order to observe the relationship between the glandular and stromal cells.

On the other hand, there have been many reports of successful transplantation of human tissues into immunodeficient mice. Nude mice, which lack a thymus and cannot generate mature T lymphocytes, were first used as recipients of xenotransplants of human adenocarcinoma of the sigmoid colon (Rygaard and Povlsen, 1969), and severe combined immunodeficiency (SCID) mice, which are deficient in both T and B lymphocytes, were used as a model of human stem-cell engraftment (McCune *et al.*, 1988). Subsequently, non-obese diabetic (NOD)-SCID mice were developed, which have a higher acceptance rate not only for neoplastic tissue but also for tissue from normal human organs. Weissman and colleagues successfully transplanted normal human ovarian cortex tissue into NOD-SCID mice and observed primordial follicle growth (Weissman *et al.*, 1999). In addition, Sato and colleagues detected by immunohistochemistry the expression of steroidogenic enzymes in NOD-SCID mice after transplantation of human ovarian grafts (Sato *et al.*, 2003). However, although these mice lack T and B lymphocytes, they do have some natural killer (NK) cell activity, which might interfere with engraftment efficiency.

Recently, NOD/SCID/γC^{null} (NOG) immunodeficient mice have been developed; these are double homozygotes for the SCID mutation and the interleukin-2 receptor γ-chain (IL-2Rγ) allelic mutation (γc^{null}). NOG mice lack both T and B lymphocytes, and are defective in NK-cell activity. This severe immunodeficiency results in high engraftment efficiency for human haematopoietic stem cells and full lineage differentiation in NOG mice (Ito *et al.*, 2002).

The aims of the present study were to culture human endometrial tissue in NOG mice, and to reproduce menstrual changes by examining their morphological and immunohistochemical features.

Materials and methods

Ethical approval

All procedures for collecting human specimens and all animal experiments were approved by the Ethics Committee of Tohoku University Graduate School of Medicine, Japan.

Animals

Mature female NOG mice aged 7–8 weeks and weighing 20–25 g were obtained from the Central Institute for Experimental Animals (Kawasaki, Japan). The animals were housed in micro-isolator cages in a barrier facility under well controlled, pathogen-free conditions. The monitored ambient temperature was 22 °C and the animals were maintained under a 12-h light/dark cycle. All housing materials were autoclaved before use. The mice were fed laboratory chow and water *ad libitum*.

Human endometrial tissue

Human endometrial tissues at the proliferative phase of the menstrual cycle were obtained from three premenopausal women (aged 35–49 years) who were undergoing hysterectomy as a result of the benign gynaecological disease, myoma uteri, at Tohoku University Hospital, Japan. Informed consent was obtained from each patient. No lesions of endometriosis were found in the abdomen of the patients during surgery. Each of the patients had a regular menstrual cycle, which had reached the early proliferative phase at the time of surgery; this was confirmed by measuring serum concentrations of 17β-estradiol (E_2) and progesterone. A sample of the endometrial tissue was fixed in 10% neutral buffered formalin, embedded in paraffin, and stained with haematoxylin and eosin in order to determine the menstrual phase according to the method of Noyes *et al.* (1950).

Fresh endometrial tissue was collected in cold sterile Dulbecco's phosphate-buffered saline, cut into fragments (diameter 2 mm) with a safety razor blade and washed twice to remove cellular debris.

Transplantation of endometrial fragments into mice

Eighteen NOG mice were placed under NEMBUTAL (Dainippon Pharmaceutical Co., Ltd, Osaka, Japan) anaesthesia by intraperitoneal injection. A small dorsolateral laparotomy was created in the abdomen of each mouse, and a bilateral ovariectomy was performed to prevent the sex hormones of the animals having an effect on the transplanted tissue. After ovariectomy, two fragments of the human endometrial tissue were transplanted into the subcutaneous space of each mouse. The ovariectomy and transplantation procedure was carried out within 3 h of hysterectomy. The treatment with sex hormones was initiated at the time of tissue transplantation. E_2 (FEMIEST; Yakult Honsha Co., Ltd, Tokyo, Japan) was administered to the mice using a transdermal patch, and progesterone (Progehormone; Mochida Pharmaceutical Co., Ltd, Tokyo, Japan) was administered by subcutaneous injection. The FEMIEST patches were cut into 0.64- or 1-cm^2 sections and attached to the backs of the mice in areas from which the fur had been removed. Mice received E_2 alone for the first 14 days (0.64 cm^2 containing 0.2 mg of E_2 for the first 7 days, and 1 cm^2 containing 0.3 mg of E_2 for the following 7 days), and E_2 (0.64 cm^2) plus progesterone (0.5 mg/kg) for the next 14 days. The patches were changed every 3 days. Hormone administration was stopped after the 28-day treatment period. All procedures were performed

under aseptic conditions in a clean-bench environment. The animals were maintained for a maximum of 35 days without antibiotics.

Histological assessment

Mice were sacrificed by removing blood from the heart under ether anaesthesia at 14, 16, 21, 28, 31 or 35 days after transplantation. The implanted endometrial fragments were extracted and fixed in 10% neutral buffered formalin for ~24 h, then embedded in paraffin. Sections (thickness 3 μm) were stained with haematoxylin and eosin for histological identification. Serum samples were measured using an enzyme-linked immunosorbent assay (Cayman Chemical Co., Ann Arbor, MI, USA).

Immunohistochemical analyses

Single immunohistochemical labelling. Immunohistochemical analyses were performed in order to demonstrate proliferative activity and to determine the type of lymphocytes that appeared in the human endometrium. The primary human antibodies used in these analyses are summarized in Table I. A HISTFINE kit (Nichirei, Tokyo, Japan) and an EnVision kit (DakoCytomation, Inc., Carpinteria, CA, USA) were used to identify the human lymphocytes. Sections (1.5 μm) were deparaffinized and treated with methanol/3% hydrogen peroxide to block endogenous peroxidase. In order to retrieve masked antigens, the slides were immersed in citrate buffer (pH 6.0) and heated in an autoclave for 5 min at 121 °C. They were then incubated with primary antibody overnight, followed by biotinylated secondary antibody for 30 min and peroxidase-labelled streptavidin for 30 min. The antigen–antibody complex was visualized with 3,3′-diaminobenzidine (DAB) solution and counterstained with haematoxylin. Positive controls were samples of endometrial cancer (Ki-67), small-cell carcinoma (CD56), thymus (CD16) and normal human lymph nodes (CD3 and CD79α). The pairs of mirror-image sections were obtained simultaneously and stained for CD56 and CD16.

Double immunohistochemical labelling. The sections of day 28 were also labelled using a sequential double immunohistochemical staining for CD56 and CD3. Sections were incubated with CD56 overnight at first and the reaction was developed with DAB. After that, sections were incubated with CD3 overnight, and the reaction was developed with 4-chloro-1-naphthol.

Results

Transplantation

All of the NOG mice that received transplants of normal human endometrial tissue into the subcutaneous space survived and were sacrificed between 14 and 35 days after surgery. The success rate of xenotransplantation was 100% and the recovery rate of fragments was 94%. The two fragments transplanted into each mouse showed similar histological changes, which were not dependent upon the patient.

Histological assessment

Before transplantation, the endometrial tissue contained numerous small narrow glands with columnar glandular cells. Evidence of pseudostratification of the nuclei was also observed. The stroma was dense, and mitotic figures were identified in both the glandular and stromal cells. These findings indicate that the endometrial tissue was in the early proliferative phase (Figure 1A).

After 14 days, the tissues contained numerous small narrow glands with columnar glandular cells and pseudostratification of the nuclei. The stroma was dense, and many mitotic figures were observed in both the glandular and stromal cells (Figure 1B). These findings suggest that the cells were actively proliferating. The mean serum concentration of E_2 was 293.1 pg/ml at this stage.

By contrast, progressive development of secretory-phase characteristics was observed after treatment commenced with progesterone plus E_2. Subnuclear vacuolation of the glandular epithelium, the first detectable feature of the secretory phase, began to appear after 2 days of E_2 plus progesterone treatment (Figure 1C). The mean serum concentrations of E_2 and progesterone were 115 pg/ml and 12.0 ng/ml, respectively. By 21 days after transplantation, the glands were noticeably dilated and filled with fluid. In addition, the glandular cells appeared cuboidal and the pseudostratification of the nuclei had disappeared. Many lymphocytes were present throughout the stroma and tended to aggregate around the glands (Figure 1D). The mean serum concentrations of E_2 and progesterone were 158 pg/ml and 19.2 ng/ml, respectively. Progressive decidual change occurred in the stroma and marked decidualization was observed 28 days after transplantation. The typical late-secretory structure was present by this stage and numerous lymphocytes were identified throughout the stroma (Figure 1E). The mean serum concentrations of E_2 and progesterone were 54.5 pg/ml and 16.5 ng/ml, respectively.

Table I. Summary of the primary antibodies used in this study

Antibody (clone number)	Source	Optimal dilution	Antigen retrieval
Ki-67 (monoclonal: MIB-1)	Dako (Glostrup, Denmark)	1:50	Autoclave[a]
CD56 (monoclonal: 123C3)	Monosan (Am uden, The Netherlands)	1:80	Autoclave[a]
CD16 (monoclonal: 2H7)	Novo Castra (Newcastle, UK)	1:160	Autoclave[a]
CD3 (polyclonal)	Dako (Glostrup, Denmark)	1:500	Autoclave[a]
CD79α (monoclonal: JCB117)	Dako (Glostrup, Denmark)	1:40	Autoclave[a]

[a]Autoclave: heat in an autoclave for 5 min in citric acid buffer.

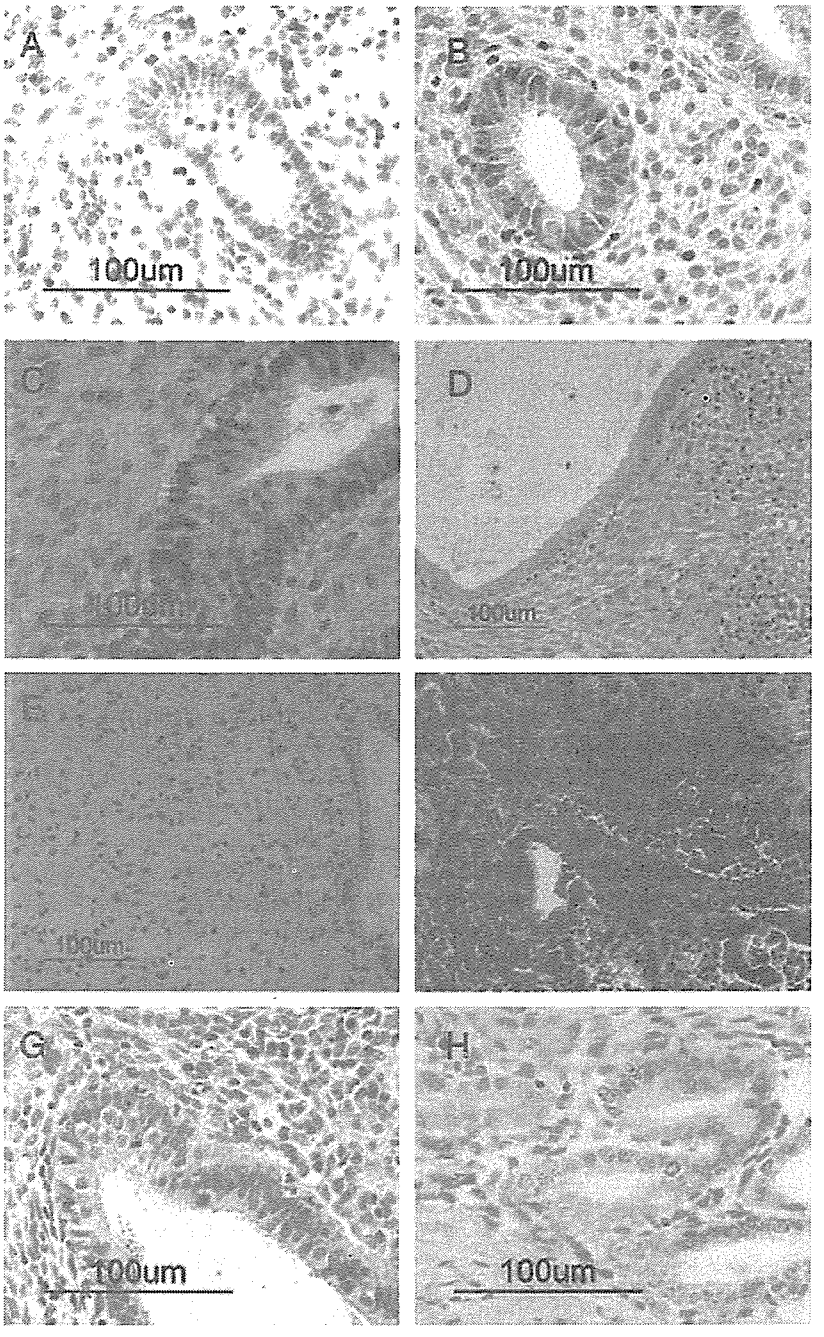

Figure 1. Histological sections stained with haematoxylin and eosin (**A–G**) and the immunohistochemical stain Ki-67 (**H**). (**A**) Pretransplantation endometrial tissue: the proliferative phase. The glands are small straight and narrow, with columnar glandular cells and prominent pseudostratification of the nuclei. The stromal cells are dense (magnification ×400). (**B**) Endometrial tissue 14 days after transplantation: E_2 has been administered for 14 days. The glands are small and narrow, with tall columnar cells. Evidence of pseudostratification of the nuclei is present. The stromal cells are dense (magnification ×400). (**C**) Endometrial tissue 16 days after transplantation: E_2 has been administered for 14 days, followed by E_2 plus progesterone for 2 days. The glands still show pseudostratified structures but they have begun to enlarge, and subnuclear vacuolation of the glandular cells is visible. The stromal cells remain dense (magnification ×400). (**D**) Endometrial tissue 21 days after transplantation: E_2 has been administered for 14 days, followed by E_2 plus progesterone for 7 days. The glands are significantly dilated, the glandular cells are cuboidal and the pseudostratification of the nuclei has disappeared. Stromal decidualization is beginning. Many lymphocytes are present throughout the stroma and are aggregating around the glands (magnification ×200). (**E**) Endometrial tissue 28 days after transplantation: E_2 has been administered for 14 days, followed by E_2 plus progesterone for 14 days. The glandular cells are cuboidal. Evidence of stromal decidualization is clearly seen and lymphocytes are present in the stroma (magnification ×200). (**F**) Endometrial tissue 31 days after transplantation: E_2 had been administered for 14 days, followed by E_2 plus progesterone for 14 days, and then no hormones for the remaining 3 days. The glands and endometrial stroma have collapsed during the evolution of the transplant. There is prominent bleeding in the stroma (magnification ×200). (**G**) Endometrial tissue 35 days after transplantation: E_2 had been administered for 14 days, followed by E_2

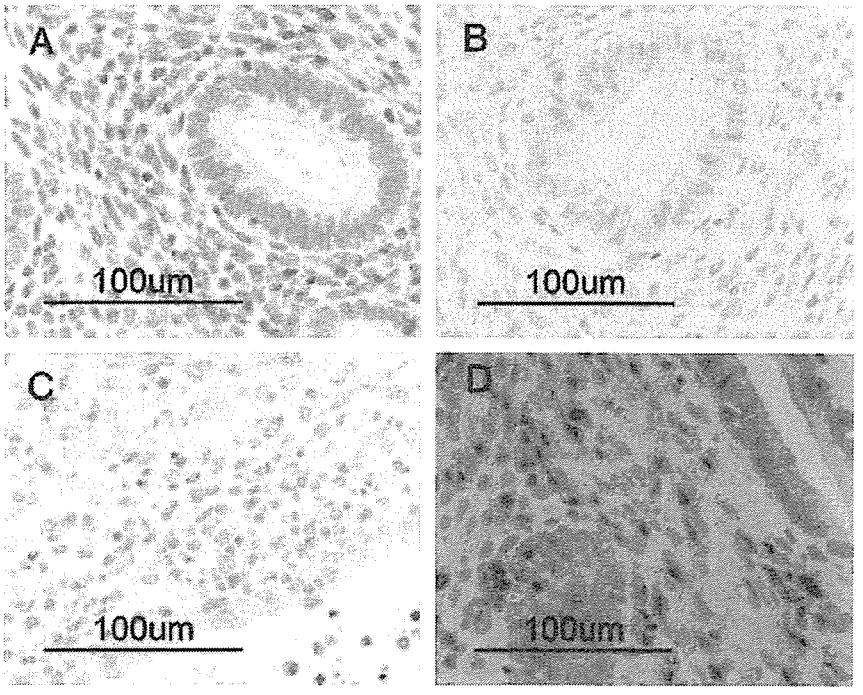

Figure 2. Immunohistochemical staining of human CD56. (**A**) Pretransplantation endometrial tissue: human CD56-positive cells are present in small numbers (magnification ×400). (**B**) Day 14 after transplantation: human CD56-positive cells have completely disappeared from the stroma (magnification ×400). (**C**) Day 21 after transplantation: human CD56-positive cells are present in small numbers (magnification ×400). (**D**) Day 28 after transplantation: human CD56-positive cells have significantly increased in number in the stroma (magnification ×400).

After 28 days hormone treatment was stopped, the decidual change ceased and tissue destruction accompanied by bleeding was observed in the stroma (Figure 1F). These findings suggest the occurrence of menstruation. By day 31, the mean serum concentrations of E_2 and progesterone were 0.9 pg/ml and 0.5 ng/ml, respectively. However, by day 35 the tissues contained many small narrow glands with columnar cells and pseudostratification of the nuclei was detected (Figure 1G). The stromal cells were dense, and mitotic figures were detected in both the glandular and stromal cells, suggesting the return of the proliferative phase.

Immunohistochemical analyses

A number of nuclei in the glandular and stromal cells were stained with Ki-67 on day 35 after transplantation (Figure 1H). Human CD56-positive cells were detected in small numbers before transplantation (Figure 2A); however, these had disappeared from the stroma by day 14 (Figure 2B). A few human CD56-positive cells were again observed in the stroma at day 21 (Figure 2C) and their numbers had significantly increased by day 28 (Figure 2D). Moderate numbers of human CD3-positive cells were detected before transplantation and at day 14; however, they had increased by days 21 and 28. Small numbers of human CD16-positive cells were detected in all specimens throughout the menstrual cycle; in contrast, human CD79a-positive cells were barely detected at any stage. Moreover, CD56-positive cells (Figure 3A) did not stain for CD16 (Figure 3B), and CD56-positive cells hardly stained for CD3 (Figure 3C) by single immunohistochemical staining of paired mirror-image sections for CD56 and CD16 and double staining for CD56 and CD3.

Discussion

We have demonstrated that human endometrial tissue transplanted into the subcutaneous space of NOG mice responded to sex-hormone treatment by showing the normal cyclical changes observed in the human endometrium. The recovery rate of the fragments was 94%, and the failures were probably caused by the transplants being too small to detect at day 35 (one contained only mouse tissue and the other only stromal tissue of human endometrium).

Several previous workers have transplanted human endometrial tissue into immunodeficient mice (Zamah *et al.*, 1984; Bergqvist *et al.*, 1985; Zaino *et al.*, 1985; Aoki *et al.*, 1994; Awwad *et al.*, 1999; Tabibzadeh *et al.*, 1999; Nisolle *et al.*, 2000a; b; Grummer *et al.*, 2001; Beliard *et al.*, 2002; Hull *et al.*, 2003). These experiments were highly variable

plus progesterone for 14 days, and then no hormones for the remaining 7 days. The glands are small and narrow with tall columnar cells. Evidence of pseudostratification of the nuclei is present. The stromal cells are dense (magnification ×400). (**H**) Endometrial tissue 35 days after transplantation: a number of nuclei have been immunohistochemically stained with Ki-67, showing proliferation of glandular and stromal cells (magnification ×400).

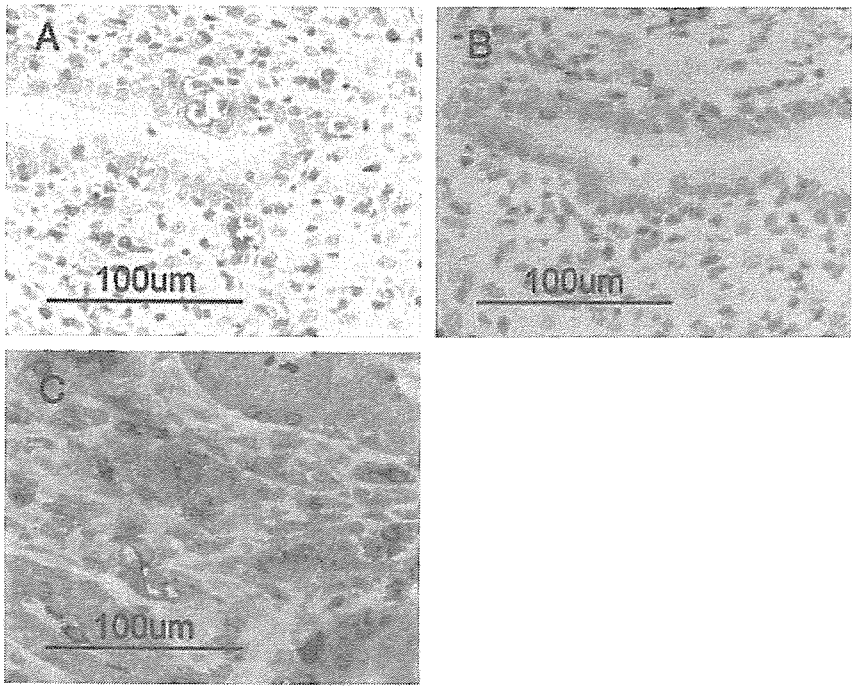

Figure 3. Paired mirror-image sections for CD56 (**A**) and CD16 (**B**), and double immunohistochemical staining section for CD56 and CD3 (**C**) at day 28: There are many CD56-positive cells in the stroma; however, they are not stained with CD16. There are many CD56-positive cells and also many CD3-positive cells in the stroma (brown deposit shows CD56-positive cells and the blue CD3-positive cells); there was minimal overlap in labelling for CD56 and CD3 (magnification ×400).

with respect to the strain of mouse used, the phase of the menstrual cycle of the transplanted tissue, the site of transplantation, whether or not ovariectomy was performed, whether or not the endometrium was pretreated and the method by which sex hormones were administered. However, despite these differences, most previous studies concluded that this system was a suitable model of endometriosis.

Zaino and colleagues transplanted human endometrial tissue into the subcutaneous space of ovariectomized athymic mice in four treatment groups (E_2, E_2 and progesterone, progesterone, and no exogenous hormone) and suggested that their model was useful for examining the histological response of normal endometrial tissue to sex hormones (Zaino *et al.*, 1985). The novelty of the approach described in the present report involves the simultaneous administration of sex steroids similar to those involved in the human menstrual cycle. Moreover, our model utilizes NOG mice that lack both T and B lymphocytes and NK-cell activity.

We observed many small narrow glands with columnar cells and pseudostratification of the nuclei in the grafted tissue 14 days after transplantation. Treatment with E_2 plus progesterone resulted in the following sequence of secretory changes in the endometrial tissue: subnuclear vacuolation and glandular secretion, followed by notable dilation of the glands, the presence of cuboidal glandular cells and the gradual decidualization of the stromal cells. This corresponds to the normal secretory phase of the endometrium. Furthermore, lymphocytes were observed during E_2 plus progesterone treatment in the mid-to-late secretory phase. After the sex-hormone treatment had ceased, tissue destruction and bleeding were observed in the stroma. We subsequently observed the reconstruction of the endometrium, the presence of small glands with columnar cells, pseudostratification of the nuclei, and mitoses in both the glandular and stromal cells. The proliferative activity was confirmed by immunohistochemistry. Ferenczy (1976) demonstrated that reconstruction of the eutopic endometrium during the early stage of the menstrual cycle is independent of ovarian hormone. Our findings suggest that the transplanted human endometrial tissue in our model returned to the proliferative phase, despite the low concentration of E_2.

The endometrial tissue in our system contained numerous lymphocytes at 21 and 28 days after transplantation. The number of large granular lymphocytes in human endometrial tissue has been reported to increase during the mid to late secretory phase, and CD56-positive, CD16-negative uterine NK cells have been identified (King *et al.*, 1989; Bulmer *et al.*, 1991; Klentzeris *et al.*, 1992) We detected small numbers of CD56-positive and CD16-negative cells on day 21, and their numbers had increased by day 28. These cells showed very little CD3 staining. It was also reported that CD3-positive cells increased from 4–7 days after the LH surge, and remained unchanged in number after that (Klentzeris *et al.*, 1992). In this model, moderate numbers of CD3-positive lymphocytes were detected at day 14; they increased on day 21 and similar numbers of these cells were detected on day 28. From these points of view, our model successfully maintained the human endometrial structure and reproduced normal menstrual changes. It is therefore suitable for studying the human endometrium both from a histological

perspective and from the appearance of lymphocytes, such as CD56-positive NK cells and CD3-positive cells.

Dallenbach-Hellweg (1971) suggested that endometrial granulated lymphocytes develop from undifferentiated endometrial stromal cells. In this study, the human CD56-positive cells that were present in the stroma before transplantation completely disappeared by day 14, reappeared at day 21 and had significantly increased in number by day 28. As the mice used in this study lacked B and T lymphocytes and NK cells, these cells could not have been derived from the peripheral blood of the mice. Therefore, there are two possibilities of the origin of CD56-positive NK cells: one is that they differentiated from the transplanted endometrial stromal cells, the other is precursor cells were located within the transplanted endometrial tissue and they arose and differentiated gradually. It could be possible to investigate the origin of the uterine NK cells by using this model; however, further studies will be necessary to clarify this issue.

We noted some differences between the transplanted tissue in our model and the normal human endometrium. Spiral arteries were not observed in the transplants after either 21 or 28 days; this was probably due to the fragmentary nature of the endometrial tissues. Normally, the uterine arteries penetrate the uterine wall and advance into the middle layer of the myometrium, where they ramify into arcuate arteries. These divide into radial arteries, which, in turn, divide into basal arteries near the myoendometrial junction. The basal arteries ascend through the stratum functionale to the endometrial surface, where they become spiral arteries. However, the transplants comprised endometrial tissue only, and lacked arcuate and radial arteries. This resulted in a different pattern of vascularization to that of normal endometrial tissues, with an absence of spiral arteries. Menstruation has long been recognized as an ischaemic necrosis of the endometrium caused by contraction of the spiral arteries due to a decrease in the levels of the sex steroid hormones (Markee, 1940; Bartelmez, 1957). However, Hoopwood and Levison (1976) reported the presence of apoptotic bodies in the human endometrium, and recent reports have also pointed to the involvement of apoptosis in the endometrium during the menstrual cycle (Tabibzadeh, 1995; Kokawa *et al.*, 1996). Igarashi *et al.*, (2001) confirmed the increase of CD56-positive cells in the late secretory phase and suggested that CD56-positive NK cells induce the apoptosis of endometrial glandular cells associated with the onset of menstruation. Marbaix *et al.*, (1996) also demonstrated *in vitro* that matrix metalloproteinases were involved in the initiation of menstruation. In the present study, bleeding and tissue destruction were observed in the stroma 31 days after transplantation. These findings suggest that our model is suitable for investigating the mechanism of menstruation in the absence of spiral arteries.

We were careful to use only natural sex steroid hormones in our model, and the appropriate periods of administration and doses were determined in a preliminary study using one piece of endometrial tissue. Interestingly, 7 days of pretreatment with E_2 followed by 14 days of E_2 plus progesterone treatment did not result in decidualization of the stromal cells, despite the administration of high E_2 and progesterone concentrations. Furthermore, after treatment with E_2 for 28 days, the transplants largely comprised dilated glands that resembled endometrial hyperplasia. Therefore, 14 days was selected as the appropriate period of E_2 administration in order to reproduce the proliferative and late secretory phases of the normal endometrium. These findings indicate that our animal model might also be useful for studying endometrial dysfunction or hyperstimulation due to under- or overexposure to estrogen.

In conclusion, we have developed a mouse model of the human menstrual hormone cycle and the recurring changes that take place in the endometrium. This novel approach may be useful for identifying the mechanism of action of steroid hormones, the origin of uterine NK cells and the mechanism of initiation of menstruation, all of which have yet to be clarified.

Acknowledgements

The authors wish to thank Drs A. Endo and S. Uehara for their kind support, and Mr S. Okamoto and Ms K. Abe for technical assistance. They also wish to thank the patients who made such a valuable contribution to this study.

References

Aoki D, Katsuki Y, Shimizu A, Kakinuma C and Nozawa S (1994) Successful heterotransplantation of human endometrium in SCID mice. Obstet Gynecol 83,220–228.

Awwad JT, Sayegh RA, Tao XJ, Hassen T, Awwad ST and Isaacsos K (1999) The SCID mouse: an experimental model for endometriosis. Hum Reprod 14,3107–3111.

Bartelmez GW (1957) The form and the functions of the uterine blood vessels in the rhesus monkey. Contrib Embryol Carnegie Inst Wash 36,153–182.

Beliard A, Noel A, Goffin F, Frankenne F and Foidart JM (2002) Role of endocrine status and cell type in adhesion of human endometrial cells to the peritoneum in nude mice. Fertil Steril 78,973–978.

Bergqvist A, Jeppsson S, Kullander S and Ljungberg O (1985) Human endometrium transplanted into nude mice. Histologic effects of various steroid hormones. Am J Pathol 119,336–344.

Bulmer JN, Morrison L, Longfellow M, Ritson A and Pace D (1991) Granulated lymphocytes in human endometrium: histochemical and immunohistochemical studies. Hum Reprod 6,791–798.

Centola GM, Cisar M and Knab DR (1984) Establishment and morphologic characterization of normal human endometrium in vitro. In Vitro 20,451–462.

Dallenbach-Hellweg G (1987) Histopathology of the Endometrium, 4th ed., Springer Verlag Berlin, Heiderberg, New york, Tokyo pp 158-200.

Ferenczy A (1976) Studies on the cytodynamics of human endometrial regeneration. II. Transmission electron microscopy and histochemistry. Am J Obstet Gynecol 124,582–595.

Finn CA, Pope MD and Milligan SR (1992) Timing of the window of uterine sensitivity to decidual stimuli in mice. Reprod Fertil Dev 4,565–571.

Flickinger GL, Elsner C, Illingworth DV, Muechler EK and Mikhail G (1977) Estrogen and progesterone receptors in the female genital tract of humans and monkeys. Ann NY Acad Sci 286,180–189.

Grummer R, Schwarzer F, Bainczyk K, Hess-Stumpp H, Regidor PA, Schindler AE and Winterhager E (2001) Peritoneal endometriosis: validation of an in-vivo model. Hum Reprod 16,1736–1743.

Heuser CH, Rock J and Hertig AT (1945) Two human embryos showing early stages of the definitive yolk sac. Contrib Embryol 201,85–99.

Hitschmann F and Adler L (1908) Der bau der uterusschleimhaut des geschlechtsreifen weibes mit besonderer berucksichtigung der menstruation. Monatsschr Geburtshilfe Gynaekol 27,1–82.

Hoopwood D and Levison DA (1976) Atrophy apoptosis in the cyclical human endometrium. J Pathol 119,159–166.

Hull ML, Charnock-Jones DS, Chan CLK, Bruner-Tran KL, Osteen KG, Tom BDM, Fan TD and Smith SK (2003) Antiangiogenesis agents are effective inhibitors of endometriosis. J Clin Endocrin Metab 88,2889–2899.

Igarashi T, Konno R, Okamoto S, Moriya T, Sato S and Yajima A (2001) Involvement of granule-mediated apoptosis in the cyclic change of the normal human endometrium. Tohoku J Exp Med 193,13–25.

Irwin JC, Kirk D, King RJ, Quigley MM and Gwatkin RB (1989) Hormonal regulation of human endometrial stromal cells in culture: an in vitro model for decidualization. Fertil Steril 52,761–768.

Ito M, Hiramatsu H, Kobayashi K, Suzue K, Kawahata M, Hioki K, Ueyama Y, Koyanagi Y, Sugawara K, Tsuji K et al. (2002) NOD/SCID/g(c)(null) mouse: an excellent recipient mouse model for engraftment of human cells. Blood 100,3175–3182.

Jensen EV and Jacobson HI (1962) Basic guides to the mechanism of estrogen action. Recent Prog Horm Res 18,387.

King A, Wellings V, Gardner L and Loke YW (1989) Immunocytochemical characterization of the unusual large granular lymphocytes in human endometrium throughout in menstrual cycle. Hum Immunol 24,195–205.

Klentzeris LD, Bulmer JN, Warren A, Morrison L, Li TC and Cooke ID (1992) Endometrial lymphoid tissue in the timed endometrial biopsy: morphometric and immunohistochemical aspects. Am J Obstet Gynecol 167,667–674.

Kokawa K, Shikone T and Nakano R (1996) Apoptosis in the human uterine endometrium during the menstrual cycle. J Clin Endocrinol Metab 81,4144–4147.

Marbaix E, Kokorine I, Moulin P, Donnez J, Eeckhout Y and Courtoy PJ (1996) Menstrual breakdown of human endometrium can be mimicked in vitro and is selectively and reversibly blocked by inhibitors of matrix metalloproteinases. Proc Natl Acad Sci USA 93,9120–9125.

Markee JE (1940) Menstruation in intraocular endometrial transplants in the rhesus monkey. Contrib Embryol Carnegie Inst Wash 28,219–308.

McCune JM, Namikawa R, Kaneshima H, Shultz LD, Lieberman M and Weissman IL (1988) The SCID-hu mouse: murine model for the analysis of human hematolymphoid differentiation and function. Science 241,1632–1639.

Nelson S (1964) The Arterial Supply of the Uterus Adnexa of the Rhesus Monkey, Master's Essays. Johns Hopkins University, Baltimore, MD, USA.

Nisolle M, Casanas-Roux F and Donnez J (2000a) Early-stage endometriosis: adhesion and growth of human menstrual endometrium in nude mice. Fertil Steril 74,306–312.

Nisolle M, Casanas-Roux F, Marbaix E, Jadoul P and Donnez J (2000b) Transplantation of cultured explants of human endometrium into nude mice. Hum Reprod 15,572–577.

Noyes RW, Hertig AT and Rock J (1950) Dating the endometrial biopsy. Fertil Steril 1,3–25.

O'Mally BW, Sherman MR and Toft DO (1970) Progesterone 'receptors' in the cytoplasm and nucleus of chick oviduct target tissue. Proc Natl Acad Sci USA 67,501–508.

Rygaard J and Povlsen CO (1969) Heterotransplantation of a human malignant tumour to 'nude' mice. Acta Path Microbiol Scand. Acta Path Microbiol Scand 77,758–760.

Sato Y, Terada Y, Utsunomiya H, Koyanagi Y, Ito M, Miyoshi I, Suzuki T, Sasano H, Murakami T, Yaegashi N et al. (2003) Immunohistochemical localization of steroidogenic enzymes in human follicle following xenotransplantation of human ovarian cortex into NOD-SCID mice. Mol Reprod Dev 65,67–72.

Sugawara J, Fukaya T, Murakami T, Yoshida H and Yajima A (1997) Hepatocyte growth factor stimulates proliferation, migration, and lumen formation of human endometrial epithelial cells in vitro. Biol Reprod 57,936–942.

Tabibzadeh S (1995) Signals and molecular pathways involved in apoptosis with special emphasis on human endometrium. Hum Reprod Update 1,303–323.

Tabibzadeh S, Miller S, Dodson WC and Satyaswaroop PG (1999) An experimental model for the endometriosis in athymic mice. Front Biosci 1,4–9.

Weissman A, Gotlieb L, Colgan T, Jurisicova A, Greenblatt EM and Casper RF (1999) Preliminary experience with subcutaneous human ovarian cortex transplantation in the NOD-SCID mouse. Biol Reprod 60,1462–1467.

Zaino RJ, Satyaswaroop PG and Mortel R (1985) Histologic response of normal human endometrium to steroid hormones in athymic mice. Hum Pathol 16,867–872.

Zamah NM, Dodson MG, Stephens LC, Buttram VC, Besch PK and Kaufman RH (1984) Transplantation of normal and ectopic human endometrial tissue into athymic nude mice. Am J Obstet Gynecol 149,591–597.

Submitted on March 9, 2004; resubmitted on October 4, 2004; accepted on January 12, 2005

AIDS RESEARCH AND HUMAN RETROVIRUSES
Volume 21, Number 4, 2005, pp. 325–330

Sequence Note

Phylogenetic Heterogeneity of new HTLV Type 1 Isolates from Southern India in Subgroup A

SADAYUKI OHKURA,[1] MASAHIRO YAMASHITA,[2] TAKAFUMI ISHIDA,[3] PALLA-GEORGE BABU,[4,†] YOSHIO KOYANAGI,[5] NAOKI YAMAMOTO,[6] TOMOYUKI MIURA,[1] and MASANORI HAYAMI[1]

ABSTRACT

Seven isolates of human T cell leukemia virus type 1 (HTLV-1) were taken in southern India and phylogenetically analyzed to gain new insights into the origin and dissemination of HTLV-1 in the subcontinent. The new Indian HTLV-1s were found to be members of subgroup A (Transcontinental subgroup) of the Cosmopolitan group. They formed three different clusters (South African/Caribbean, Middle Eastern, and East Asian clusters). These results demonstrate that Indian HTLV-1s are genetically heterogeneous and include the most divergent strain of subgroup A. On the basis of these results, we speculate that subgroup A HTLV-1s may have been present for thousands of years in India.

HUMAN T CELL LEUKEMIA VIRUS type 1 (HTLV-1) is the causative agent of adult T cell leukemia (ATL) and HTLV-1-associated myelopathy/tropical spastic paraparesis (HAM/TSP).[1–3] HTLV-1 has unique geographic and ethnologic distribution patterns. It is endemic mainly in Melanesia, the Caribbean basin, sub-Saharan Africa, and southwestern Japan and is highly prevalent among certain ethnic populations including Jews in Iran, the Ainu in Japan, Aboriginals in Australia, and Native Americans. These sporadic infections are thought to be vestiges of various migrations of HTLV-1 carriers from endemic areas, although how this distribution was established is not clear.

Seroepidemiological surveys have shown sporadic HTLV-1 infections in India. In a previous phylogenetic study,[4] Indian HTLV-1s were found to belong to the phylogenetic group that includes the Middle Eastern HTLV-1 strains, suggesting a possible link between these two areas. However, from that work it was unclear whether Indian HTLV-1 strains are indeed the closest to Middle Eastern strains, because clear phylogenetic separation of HTLV-1 strains could not be accomplished on the basis of the protein-encoding regions (*gag*, *pol*, *env*, and *pX* genes) analyzed in the previous work. In contrast to analyses based on these regions, analysis of the long terminal repeats (LTR) region permits finer separation of taxa within the genotype that includes Indian and Middle Eastern HTLV-1s. Thus, to gain new insights into the origin and dissemination of HTLV-1 in India, we phylogenetically analyzed seven new HTLV-1s from southern India on the basis of the LTR region.

The prevalence of HTLV-1 in southern India was examined by serological assays. Sera were collected in three districts of southern India (Kerala, Andhra Pradesh, and Tamil Nadu), and were tested by a particle agglutination (PA) test (Serodia HTLV-1; Fujirebio, Tokyo, Japan). Reactive sera in the PA test were further confirmed by an immunofluorescence assay as described previously.[2] Three serum samples were collected from Dravidian speakers living in Andhra Pradesh in southern India (Table 1) and phylogenetically analyzed. In addition, we analyzed HTLV-1s of four reported seropositives (two from the

[1]Laboratory of Primate Model, Experimental Research Center for Infectious Diseases, Institute for Virus Research, Kyoto University, Kyoto 606-8507, Japan.
[2]Divisions of Human Biology and Basic Sciences, Fred Hutchinson Cancer Research Center, Seattle, Washington.
[3]Department of Biological Sciences, Graduate School of Science, University of Tokyo, Tokyo, Japan.
[4]Christian Medical College Hospital, Tamil Nadu, India.
[5]Laboratory of Viral Pathogenesis, Institute for Virus Research, Kyoto University, Kyoto, Japan.
[6]Department of Molecular Virology, School of Medicine, Tokyo Medical and Dental University, Tokyo, Japan.
[†]We are deeply saddened to report that Palla-George Babu died in a traffic accident.

TABLE 1. SEVEN HTLV-1s ISOLATED FROM SOUTHERN INDIA IN THIS STUDY

HTLV-1 isolate	*Place*	*Age (years)*	*Sex*	*Disease*	*Subject*			*Notes*
					PA[a]	*Western blot*	*IFA*	
AP15	Andhra Pradesh	60s	M	Nervous disease	NI	NI	NI	Inhabits inland near the Tamil Nadu district
IND001	Andhra Pradesh	NI	F	NI	+	NI	NI	
IND002	Andhra Pradesh	11	NI	NI	NI	NI	NI	Blood sample on filter paper
IN2	Kerala	47	F	NI	NI	NI	NI	Wife of the subject from whom IN3 was isolated
IN3	Kerala	52	M	ATL	+(16)	+	+	A migrant worker in the Middle East
Ma1	Tamil Nadu	20	F	ARC	+(8192)	Not done	+	Also positive for HIV-1
TNA	Tamil Nadu	43	F	NI	+(512)	NI	NI	Also positive for HIV-1

Abbreviations: ARC, AIDS-related complex; ATL, adult T cell leukemia; IFA, immunofluorescence assay; NI, no information available; PA, particle agglutination test.
[a]Figures in parentheses represent the titer of HTLV-1 antibodies.

Tamil Nadu district[5] and the other two from the Kerala district[6]) (Table 1). The two seropositives from Kerala were also Dravidian speakers. Two of the three Andhra Pradesh subjects (from whom IND001 and IND002 were isolated) said that they had had blood transfusions. It is unknown whether the other five subjects had received blood transfusions. Of the two Tamil Nadu subjects, the one from whom TNA was isolated was a commercial sexual worker and the one from whom Ma1 was isolated had sexual contacts with prostitutes.

For all but one of the subjects, chromosomal DNA (containing HTLV-1 proviral DNA) was extracted from either cultured or uncultured peripheral blood mononuclear cells (PBMCs) by a standard procedure with proteinase K. For the subject from whom IND002 was isolated, chromosomal DNA was extracted from whole blood that was blotted onto filter paper.[4] Randomly selected regions (approximately 1 cm^2) of the filter paper were cut into more than 100 pieces with sterile scissors. The pieces were put into 3 ml of 0.85% NaCl solution and shaken at room temperature for 1 hr. Supernatants were centrifuged for 1 min to precipitate free PBMCs, which were utilized for the subsequent extraction of DNA.

The extracted DNA was subjected to nested polymerase chain reaction (PCR) to amplify a part of the LTR region that corresponds to nucleotide positions 99 to 685 of ATK, a prototypic Japanese HTLV-1 strain, with special care to avoid cross-contamination of the amplified products as described previously.[7] Throughout this study, all negative controls gave negative signals. Nucleotide sequences of a part of the amplified LTR fragments that correspond to positions 122 to 628 of ATK were determined in both directions, using an automated DNA sequencer (Applied Biosystems, Foster City, CA). Nucleotide sequences were aligned with the computer software CLUSTAL W with minor manual modifications. Phylogenetic trees were constructed by the neighbor-joining (NJ) method. For construction of NJ trees, bootstrapping was done to generate 1000 resamplings of the original sequence alignments, and pairwise genetic distances were estimated on each resampling by the Kimura two-parameter method. Phylogenetic trees were then constructed with CLUSTAL W and the trees were visualized by TREEVIEW. Detailed procedures and references for construction of the trees are described elsewhere.[7] The GenBank accession numbers for the new strains are AY607576 to AY607582.

We amplified a part of the LTR region of seven new HTLV-1s from India (Table 1). HTLV-1 isolates are phylogenetically separated into three major genotypes. Most HTLV-1 isolates from the world form a large group called the Cosmopolitan group or HTLV-1a. HTLV-1 isolates from Central Africa and those from Melanesia have diverged from those of the Cosmopolitan group, and are thus collectively called the Central African (HTLV-1b and -1d) and Melanesian (HTLV-1c) groups, respectively. The LTR sequences of the newly isolated HTLV-1s exhibited higher genetic similarities to HTLV-1 strains of the Cosmopolitan group (97.1%) than to those of the Central African (94.4%) and Melanesian groups (91.3%). The phylogenetic analysis also placed the newly isolated HTLV-1s into the Cosmopolitan group (Fig. 1). This group has been divided into five subgroups (A to E) on the basis of their LTR sequences. Each of the five subgroups closely correlates with the geographic origins of its HTLV-1 isolates. According to our data (Fig. 1), all of the new HTLV-1 strains belong to subgroup A (Transcontinental subgroup). This was confirmed by their restriction fragment length polymorphism (RFLP) profiles, which are consistent with those of subgroup A in our classification. Namely, the analyzed LTR fragments of the new HTLV-1s have *Nde*I and *Sac*I sites, but not *Dra*I and *Mae*III sites, which is consistent with the RFLP patterns of subgroup A strains. All of these data demonstrate that the prevalent genotype of HTLV-1 in southern India is subgroup A of the Cosmopolitan group.

Because all of the new Indian isolates belong to subgroup A (Fig. 1), their nucleotide alignments were compared with those of subgroup A strains. The new strains formed three different clusters (Fig. 2). One cluster contained two of the new strains (IND001 and IND002) together with South African and Caribbean HTLV-1s (Caribbean/South African/Indian cluster). Another cluster contained two other Indian HTLV-1s (AP15 and TNA) together with mostly Middle Eastern HTLV-1s (Middle Eastern cluster). The third cluster contained the other three Indian isolates (IN2, IN3, and Ma1) together with Japanese HTLV-1 strains. We tentatively refer to this cluster as the East Asian cluster. These clusters had the following characteristic nucleotide substitutions: HTLV-1s of the Caribbean/South African/Indian cluster have a G-to-A substitution at nucleotide position 246 in ATK, a C-to-T substitution at position 386, and an A-to-G substitution at position 575. Two of the Indian isolates (AP5 and TNA), like strains of the Middle Eastern cluster, have G rather than A at 240. It is noteworthy that within subgroup A, AP15 and TNA were phylogenetically located at the nodes of the Middle Eastern cluster, while Ma1 was branched off at the node of the East Asian cluster (Fig. 2). Collectively, these results indicate that subgroup A HTLV-1s circulating in India are polyphyletic.

The finding that HTLV-1s in southern India formed three different clusters indicates that the HTLV-1s of southern India are highly heterogeneous. This heterogeneity is in sharp contrast to the homogeneity of subgroup A HTLV-1s from other geographic areas. For example, HTLV-1s of South America and the Middle East form respective clusters (the Latin American and Middle Eastern clusters) within subgroup A. In addition, as shown in Fig. 1, India has the most divergent strain of subgroup A (SG).[8,9] The present analysis further showed that within subgroup A, some of the new Indian HTLV-1s are phylogenetically located at or branched off the node of the Middle Eastern and East Asian clusters. As a result, subgroup A HTLV-1s in southern India are clearly distinguishable from those of other geographic areas in that southern India has both the most divergent HTLV-1 and highly heterogeneous HTLV-1s.

These findings have an interesting implication with respect to the origin of HTLV-1 in India. Earlier studies hypothesized that HTLV-1 was introduced into India by recently migrated peoples such as African slaves several hundreds years ago, or by Jewish populations that migrated from the Middle East about 1000 to 1300 years ago.[4] However, our results indicate that Indian HTLV-1 is much more heterogeneous and includes more divergent strains than subgroup A HTLV-1 of other geographic origins such as Africa and the Middle East. This implies that HTLV-1 has been present in India for much longer than 1300 years.

If this is correct, how did HTLV-1 get to India? HTLV-1 isolates analyzed in the present study were isolated from the Dravidians, a population that migrated to India several thousand years ago. The high heterogeneity and divergence of HTLV-1 in southern India may be explained by the genetic vari-

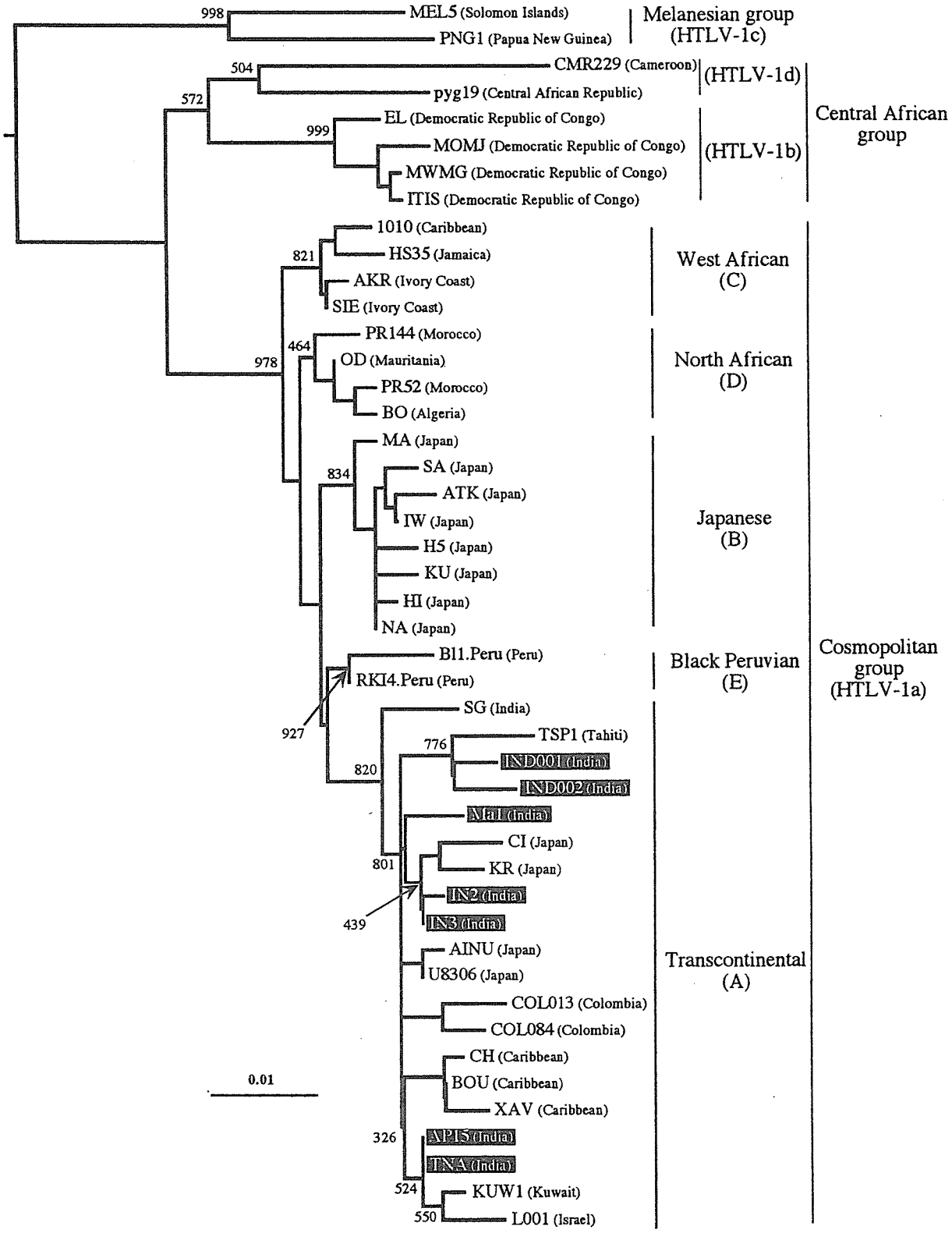

FIG. 1. Phylogenetic tree of HTLV-1 isolates based on a part of the LTR region (nucleotide positions 122–628 in ATK), showing the evolutionary relationships between the new isolates from India and isolates previously reported. Newly isolated HTLV-1s from India are highlighted. The tree was constructed by using the neighbor-joining (NJ) method. The scale at the bottom of the tree indicates the number of nucleotide substitutions per site. The horizontal branch lengths are proportional to the genetic distance. Numbers at nodes are bootstrap values. The tree was rooted with a prototype isolate of HTLV-2, MoT. The other DNA sequences used for construction of the phylogenetic tree have been described previously.[7]